JCI The Journal of Clinical Investigation

β-Catenin–regulated myeloid cell adhesion and migration determine wound healing

Saeid Amini-Nik, … , Boris Hinz, Benjamin A. Alman

J Clin Invest. 2014;124(6):2599-2610. https://doi.org/10.1172/JCI62059.

Research Article **Immunology**

A β-catenin/T cell factor–dependent transcriptional program is critical during cutaneous wound repair for the regulation of scar size; however, the relative contribution of β-catenin activity and function in specific cell types in the granulation tissue during the healing process is unknown. Here, cell lineage tracing revealed that cells in which β-catenin is transcriptionally active express a gene profile that is characteristic of the myeloid lineage. Mice harboring a macrophage-specific deletion of the gene encoding β-catenin exhibited insufficient skin wound healing due to macrophage-specific defects in migration, adhesion to fibroblasts, and ability to produce TGF-β1. In irradiated mice, only macrophages expressing β-catenin were able to rescue wound-healing deficiency. Evaluation of scar tissue collected from patients with hypertrophic and normal scars revealed a correlation between the number of macrophages within the wound, β-catenin levels, and cellularity. Our data indicate that β-catenin regulates myeloid cell motility and adhesion and that β-catenin–mediated macrophage motility contributes to the number of mesenchymal cells and ultimate scar size following cutaneous injury.

β-Catenin–regulated myeloid cell adhesion and migration determine wound healing

Saeid Amini-Nik,[1] Elizabeth Cambridge,[2] Winston Yu,[1] Anne Guo,[1] Heather Whetstone,[1] Puviindran Nadesan,[1] Raymond Poon,[1] Boris Hinz,[2] and Benjamin A. Alman[1,3]

[1]Program in Developmental and Stem Cell Biology, The Hospital for Sick Children, Peter Gilgan Center for Research and Learning, Toronto, Ontario, Canada.
[2]Laboratory of Tissue Repair and Regeneration, Matrix Dynamics Group, Faculty of Dentistry, University of Toronto, Toronto, Ontario, Canada.
[3]Department of Orthopedic Surgery, Duke University, Durham, North Carolina, USA.

A β-catenin/T cell factor–dependent transcriptional program is critical during cutaneous wound repair for the regulation of scar size; however, the relative contribution of β-catenin activity and function in specific cell types in the granulation tissue during the healing process is unknown. Here, cell lineage tracing revealed that cells in which β-catenin is transcriptionally active express a gene profile that is characteristic of the myeloid lineage. Mice harboring a macrophage-specific deletion of the gene encoding β-catenin exhibited insufficient skin wound healing due to macrophage-specific defects in migration, adhesion to fibroblasts, and ability to produce TGF-β1. In irradiated mice, only macrophages expressing β-catenin were able to rescue wound-healing deficiency. Evaluation of scar tissue collected from patients with hypertrophic and normal scars revealed a correlation between the number of macrophages within the wound, β-catenin levels, and cellularity. Our data indicate that β-catenin regulates myeloid cell motility and adhesion and that β-catenin–mediated macrophage motility contributes to the number of mesenchymal cells and ultimate scar size following cutaneous injury.

Introduction

When the protective barrier of the skin is damaged, an intricate process of tissue repair is set in motion that involves multiple cell types and signaling pathways. Three percent of the population suffers from disordered wound repair (1, 2). Insufficient or excessive healing responses result in either a nonhealing wound or formation of a hypertrophic scar, respectively. Both conditions have major deleterious effects, resulting in morbidity from loss of function, negative psychosocial effects from disfigurement, or even mortality from the loss of the skin's barrier function. Physiological wound healing is divided into the sequential, yet overlapping, stages of hemostasis, inflammation, proliferation, and remodeling (3, 4). The proliferative phase is characterized by granulation tissue formation, collagen deposition, reepithelialization, and wound contraction. Because skin does not completely regenerate, scar formation is the consequence of normal skin injury repair (3, 5, 6). A variety of different cell types, including macrophages, fibroblasts, and contractile myofibroblasts, participate in the proliferative phase of wound repair and play a critical role in regulating the size and quality of the scar that ultimately forms (7–9).

β-Catenin, a key mediator in the canonical Wnt signaling pathway, plays a prominent role during the proliferative phase of wound repair (5, 10, 11). Canonical Wnt signaling is mediated by a multi-protein complex, including glycogen synthase kinase-3 (GSK-3β), which targets β-catenin for ubiquitin-mediated degradation (12). Inhibition of ubiquitin-mediated β-catenin degradation results in the cytoplasmic accumulation and subsequent nuclear translocation of β-catenin. Binding of β-catenin to T cell factors (Tcfs) in the nucleus forms a transcriptional activation complex that induces the expression of cell type–specific target genes, ultimately regulating the size of the scar remaining after wound repair (13). We previously showed that a subset of cells in the wound granulation tissue exhibit increased β-catenin/Tcf–mediated transcriptional activity, which returns to baseline following the proliferative phase (5). However, the relative contribution of β-catenin signaling in specific cell types in wound repair is not completely elucidated.

Myeloid cells can exist as circulating monocytes and as tissue macrophages that contribute to hemostasis, inflammation, and acquired immunity (14, 15). Macrophage cells play a critical role in wound repair, since in their absence there is a near-complete lack of accumulation of granulation tissue (14–20). However, the regulation and function of myeloid lineage cells during the repair process are not known. Here, we show that wound granulation tissue cells with active β-catenin/Tcf transcription express marker genes for macrophages. Using genetically modified mice and cell lineage–tracing studies, we show that β-catenin in macrophages is essential for normal wound repair by regulating macrophage cell motility and adhesion, ultimately controlling the recruitment of the critical cells responsible for normal repair into the wound bed.

Results

Genes that are characteristically expressed by macrophages are upregulated in Tcf transcriptionally active cells during skin healing. To identify the cell types in which β-catenin/Tcf signaling is activated during skin wound healing, we examined the repair of full-thickness wounds in Tcf reporter mice (5, 21). In these mice, Tcf-mediated transcription activated the expression of *lacZ*, which we detected in 7-day-old wound granulation tissue using β-gal staining (Figure 1A). Cells were dissociated from the granulation tissue and sorted into β-gal–positive and –negative cells by FACS using fluorescein di-β-D-galactopyranoside (FDG) (22). Comparison of gene expression between both populations using the Affymetrix mouse

Conflict of interest: The authors have declared that no conflict of interest exists.

Note regarding evaluation of this manuscript: Manuscripts authored by scientists associated with Duke University, The University of North Carolina at Chapel Hill, Duke-NUS, and the Sanford-Burnham Medical Research Institute are handled not by members of the editorial board but rather by the science editors, who consult with selected external editors and reviewers.

Citation for this article: *J Clin Invest.* 2014;124(6):2599–2610. doi:10.1172/JCI62059.

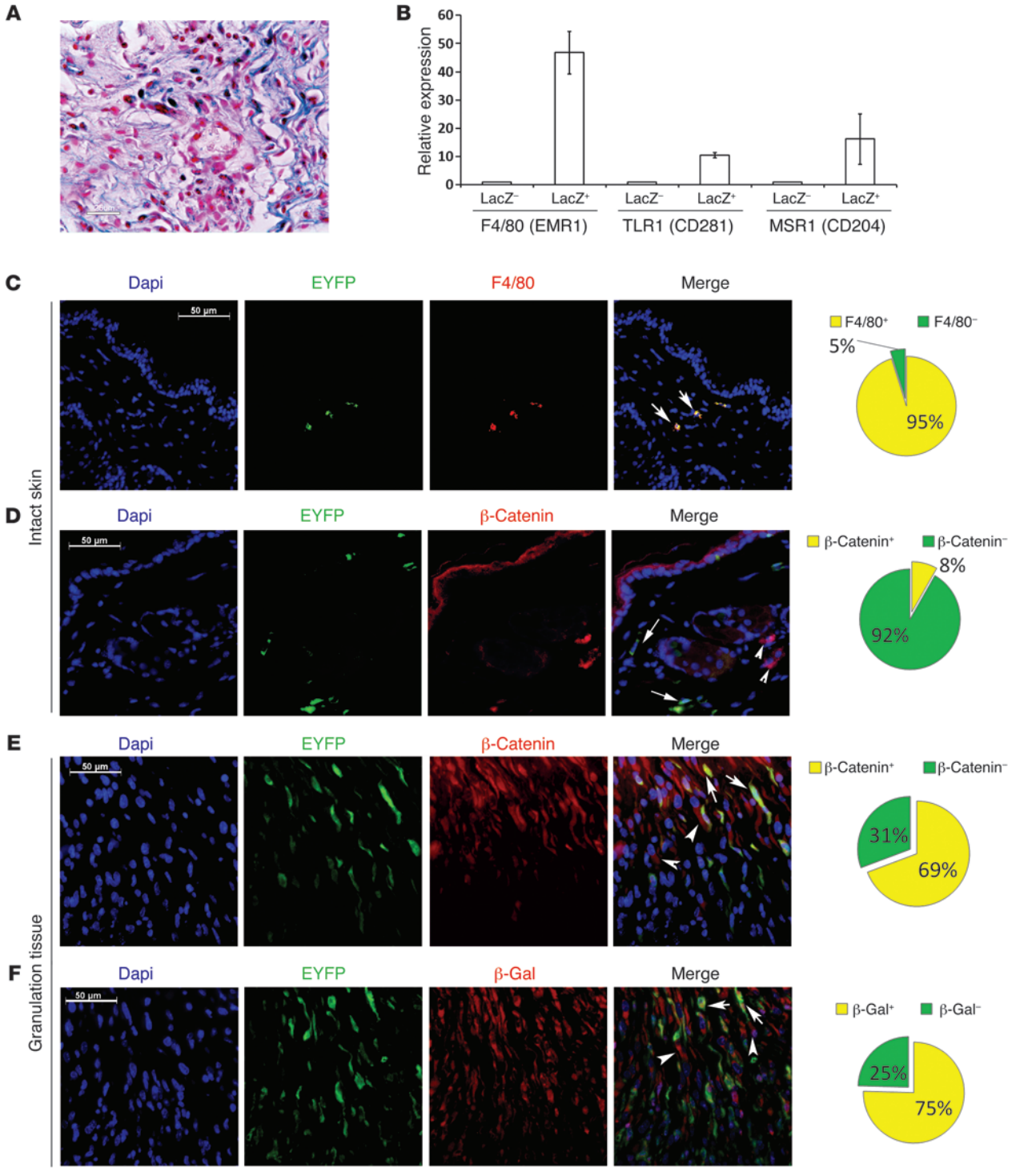
A
B
Relative expression
60
50
40
30
20
10
0
LacZ⁻
LacZ⁺
LacZ⁻
LacZ⁺
LacZ⁻
LacZ⁺
F4/80 (EMR1)
TLR1 (CD281)
MSR1 (CD204)
C
Dapi
EYFP
F4/80
Merge
50 μm
F4/80⁺
F4/80⁻
5%
95%
Intact skin
D
Dapi
EYFP
β-Catenin
Merge
50 μm
β-Catenin⁺
β-Catenin⁻
8%
92%
E
Dapi
EYFP
β-Catenin
Merge
50 μm
β-Catenin⁺
β-Catenin⁻
31%
69%
Granulation tissue
F
Dapi
EYFP
β-Gal
Merge
50 μm
β-Gal⁺
β-Gal⁻
25%
75%

Figure 1
Tcf transcriptionally active cells express genes characteristic of macrophages during skin healing. (**A**) Dermal component of a healing wound in a Tcf reporter mouse showing a subpopulation of fibroblast-like cells that were transcriptionally active for β-catenin/Tcf labeled with β-gal. Scale bar: 26 μm. (**B**) Quantitative RT-PCR analysis showing a higher expression level of genes known to be expressed in macrophages in β-gal–positive cells compared with expression levels of these genes in β-gal–negative cells. Data are shown as the mean ± 95% CI of results from 8 mice. (**C**) Double immunofluorescence staining of intact skin from a *Lysz-Cre ROSA-EYFP* mouse showing that EYFP-positive cells were also positive for F4/80. Arrows indicate EYFP-positive myeloid cells. In unwounded mice, EYFP-positive cells were also positive for F4/80. (**D**) Double immunofluorescence staining of intact skin from a *Lysz-Cre ROSA-EYFP* mouse showing that macrophages (EYFP-positive cells) in the unwounded skin did not express β-catenin. Arrows show EYFP-positive cells, and arrowheads show EYFP- and β-catenin–positive cells. (**E**) Double immunofluorescence staining of granulation tissue of healing wounds from a *Lysz-Cre ROSA-EYFP* mouse showing colocalization of EYFP and β-catenin in EYFP-positive cells. Arrows show EYFP-positive/β-catenin–positive cells, and arrowheads show EYFP-negative/β-catenin–positive cells, indicating that β-catenin was expressed in myeloid cells during the healing process. (**F**) Double immunofluorescence staining of the wound granulation tissue from a *Lysz-Cre ROSA-EYFP* Tcf mouse showing colocalization of EYFP and β-gal. Arrows show EYFP-positive/β-gal–positive cells, and arrowheads show EYFP-negative/β-gal–positive cells, indicating that myeloid cells exhibited β-catenin–dependent Tcf-mediated transcriptional activity during healing. (**C**–**F**) Pie charts illustrating the proportion of positive and negative stained cells in samples from 8 mice. Scale bars: 50 μm.

1.0 ST gene array analyzed with Ingenuity pathway analysis (23) identified the activation of macrophage markers and pathways in the β-gal–positive cell population (Supplemental Table 1, Gene Expression Omnibus [GEO] database, GEO GSE30913; supplemental material available online with this article; doi:10.1172/JCI62059DS1). Real-time PCR confirmed that cells with active β-catenin/Tcf signaling exhibited markedly higher expression of the macrophage markers F4/80, CD281, and CD204 compared with the Tcf-inactive population (Figure 1B).

Lysozyme-expressing progeny cells account for 18% of cells in the healing dermis and are active for β-catenin–mediated Tcf-dependent signaling. To further examine the specific contribution of macrophages to wound repair, we generated mice that permanently express enhanced yellow fluorescent protein (EYFP) under control of the lysozyme (*Lysz*) promoter (*Lysz-Cre ROSA-EYFP* mice, Supplemental Figure 1 and Supplemental Figure 2). Lysozyme is expressed in myeloid cells, including monocytes and macrophages (24). The skin of the unwounded *Lysz-Cre ROSA-EYFP* mice contained only a small proportion (2.1 ± 0.95%, 95% CI) of EYFP-positive cells. In the intact skin, EYFP-positive cells were almost all positive for the macrophage marker F4/80 (Figure 1C), showing the specificity of the EYFP in identifying myeloid lineage cells. The EYFP-positive cells in the intact skin rarely exhibited nuclear β-catenin staining (8 ± 7% of cells, Figure 1D). In contrast, 69 ± 17% of EYFP-positive cells in the granulation tissue of healing wounds exhibited nuclear β-catenin staining (Figure 1E). Next, we crossed *Lysz-Cre ROSA*-EYFP mice with Tcf LacZ reporter mice (*Lysz-Cre ROSA-EYFP* Tcf, Supplemental Figure 1). Quantification of 7-day-old wound granulation tissue for cells double-positive for EYFP and β-gal expression demonstrated that 75 ± 18% of myeloid cells or their progeny had active β-catenin/Tcf signaling (Figure 1F). EYFP-positive cells were substantially enriched in the granulation tissue as compared with those see in the neighboring intact skin (Figure 2, A–C). Analysis of cells from the wounds using flow cytometry showed that EYFP-positive cells accounted for 18 ± 6% of all cells in the granulation tissue (Figure 2, D and E). EYFP-positive cells persisted at 4 weeks after wounding and accounted for 11 ± 6% of the cells in the scar tissue at this later time point (Supplemental Figure 5). Thus, β-catenin–mediated Tcf-dependent signaling was active in the majority of myeloid lineage cells present during proliferative phase of dermal skin, and these cell accounted for a substantial proportion of cells present in early wound repair.

β-Catenin in myeloid lineage cells has an essential role during skin healing. To investigate the functional role of β-catenin in myeloid cells, we crossed *Lysz-Cre ROSA-EYFP* mice with mice expressing the *Catnb*^{tm2KEM} allele (*Lysz-Cre Catnb*^{tm2KEM} *ROSA-EYFP* mice; Supplemental Figure 3). In these mice, β-catenin was specifically eliminated in the EYFP-positive myeloid cells. In contrast to normally healing, full-thickness cutaneous wounds in control *Lysz-Cre ROSA-EYFP* mice (Figure 3A), wounds in mice with the myeloid-specific β-catenin knock down lacked closure of the wound 1 week after injury, as demonstrated by incomplete converged keratinocytes and a near-complete lack of granulation tissue at this time point (Figure 3B, quantified in Figure 3, C and D, and in Supplemental Figure 3D). This wound-healing phenotype is reminiscent of the phenotype observed in mice lacking macrophages (16, 17). Since recombination efficiency may not have been complete, we examined whether there was a relationship between recombination efficiency and the wound phenotype. Since wounds from mice in which macrophages lacked β-catenin showed very little granulation tissue, we examined recombination efficiency in macrophages in the bone marrow. There was a negative correlation between the extent of recombination (percentage of bone marrow–derived EYFP-positive macrophages in *Lysz-Cre Catnb*^{tm2KEM} *ROSA-EYFP* mice) and the number of cells in the granulation tissue (r = –0.865, Pearson's correlation, P value < 0.014) (Figure 3E). In mice lacking β-catenin in macrophages, the scar was immature and retained proliferation-phase characteristics 4 weeks after wounding. Aniline blue staining demonstrated lower levels of collagen and hypercellularity in wounds of *Lysz-Cre Catnb*^{tm2KEM} *ROSA-EYFP* mice compared with levels in control mice. Using a collagen deposition score, the control mice were found to have more collagen deposition in their wounds (9.8 ± 3.4 in control mice versus 4.6 ± 2.9 in *Lysz-Cre Catnb*^{tm2KEM} *ROSA-EYFP* mice) 4 weeks after wounding. Mice lacking β-catenin in macrophages showed defective cutaneous repair kinetics and deficient ultimate healing.

Macrophages lacking β-catenin cannot rescue deficient skin healing. To determine the function of β-catenin in macrophages during pathologic wound repair, we examined healing in the mice that were irradiated at sublethal doses (2.6 Gy 24 hours before wounding). Wounds in these mice lacked macrophages and had a phenotype reminiscent of that seen in macrophage-deficient mice (refs. 25, 26, and Figure 4A, magnified in Figure 4D). Control or β-catenin–deficient macrophages harvested from bone marrow were applied to the wounds of irradiated mice. Control macrophages, which can be detected by red fluorescent protein (RFP) expression, substantially improved skin wound healing and increased the number of cells present in the 7-day-old wound granulation tissue (Figure 4B, magnified in E). Flow cytometry of cells from the granulation tissue of the irradiated mice showed RFP$^+$ cells in the wounds (Figure 4H). In contrast, β-catenin–deficient macro-

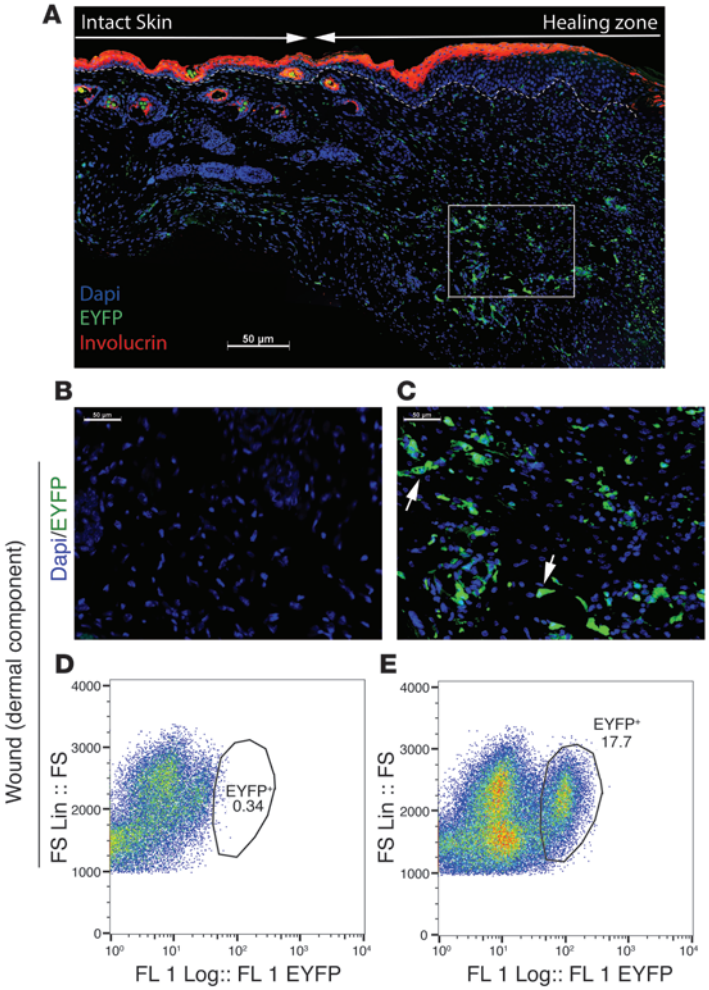

Figure 2
Lysz-expressing myeloid cells contribute to the dermal compartment of wound repair. (**A**) Low-magnification image of the entire wound from a *Lysz-Cre ROSA-EYFP* mouse showing the granulation tissue and surrounding intact skin. Involucrin (marker of the differentiated upper layer of a keratinocyte) is stained red. Dashed line separates the keratinocyte zone from the lower dermis layer. Arrows separate the intact skin from the healing zone. (**B**) Fluorescence microscopy of the healing tissue in a *ROSA-EYFP* control mouse showing the absence of EYFP-positive cells. (**C**) Fluorescence microscopy of a 7-day-old wound from a *Lysz-Cre ROSA-EYFP* reporter mouse showing that a subpopulation of cells were EYFP positive. (**D**) Flow cytometric analysis of the granulation tissue from a control *ROSA-EYFP* mouse. (**E**) Flow cytometric analysis of healing tissue in a *Lysz-Cre ROSA-EYFP* mouse showing that 18% of cells were EYFP positive (Lysz-expressing progeny) in healing skin. (**A**–**C**) Scale bars: 50 μm. FS, forward scatter; FS Lin: forward scatter on linear scatter; FL1, first fluorescent detector.

phages were not able to restore normal healing of the wounds that were devoid of granulation tissue cells (Figure 4C, magnified in Figure 4F; total cell number is quantified in Figure 4I). This raises the possibility that macrophages lacking β-catenin are deficient in their ability to migrate to the healing wound (Figure 4G).

β-*Catenin regulates genes implicated in cell migration and adhesion in macrophages*. Since β-catenin regulates gene expression, we performed gene profiling using the Affymetrix mouse 1.0 ST cDNA gene array to determine the function of β-catenin in macrophage cells. Compared with control macrophages, β-catenin–deficient macrophages showed decreased expression of numerous genes with functions attributed to migration and adhesion, including members of the cadherin, integrin, and a disintegrin and metalloproteinase (ADAM) gene families (Gene Expression Omnibus database, GEO GSE52163) (Supplemental Table 2). Cadherins and catenins are important for macrophage cell contact (27–31), whereas ADAMs and integrins are important for macrophage cell migration (32). More than 50% of ADAM and integrin gene family members showed lower expression levels in macrophages from *Lysz-Cre Catnb*^{tm2KEM} mice compared with those observed in control macrophages (Supplemental Table 3 and Supplemental Table 4).

β-*Catenin regulates macrophage cell adhesion to fibroblasts*. The data from gene expression profiling and from the treatment of irradiated wounds suggest that that β-catenin regulates macrophage cell migration and/or adhesion. Thus, we next examined the characteristics of macrophage adhesion to fibroblastic cells. Macrophages obtained from *Lysz-Cre Catnb*^{tm2KEM} *ROSA-EYFP* and control *Catnb*^{tm2KEM} *ROSA-EYFP* mouse bone marrow were seeded onto monolayers of cultured fibroblasts that do not express the conditional β-catenin allele. Macrophages deficient in β-catenin showed a smaller number of cells adhering to fibroblasts (80 ± 8% versus 57 ± 16%) compared with those seen in control macrophages (Figure 5). Scanning electron microscopy showed that β-catenin–deficient macrophages formed fewer (24 ± 6% vs. 14 ± 7%) and shorter pseudopod projections when adhering to the fibroblast layer ($P < 0.043$) (Figure 5E) compared with those in control macrophages (Figure 5B). Since cadherins and catenins are important for macrophage cell contact (27–31), we examined the expression of α-catenin and cadherin-2 (N-cadherin). Quantitative PCR demonstrated a significant decrease in α-catenin and cadherin-2 expression in macrophages lacking β-catenin compared with macrophages from control littermates (Figure 5H). β-catenin plays a role in macrophage adhesion to fibroblasts, and this adhesion is likely important for the ability of reparative myeloid lineage cells to be retained in the wound granulation tissue.

Macrophages lacking β-*catenin are impaired in their ability to migrate*. To determine the role of β-catenin in macrophage motility, we used an in vitro monolayer scratch assay. Macrophages lacking

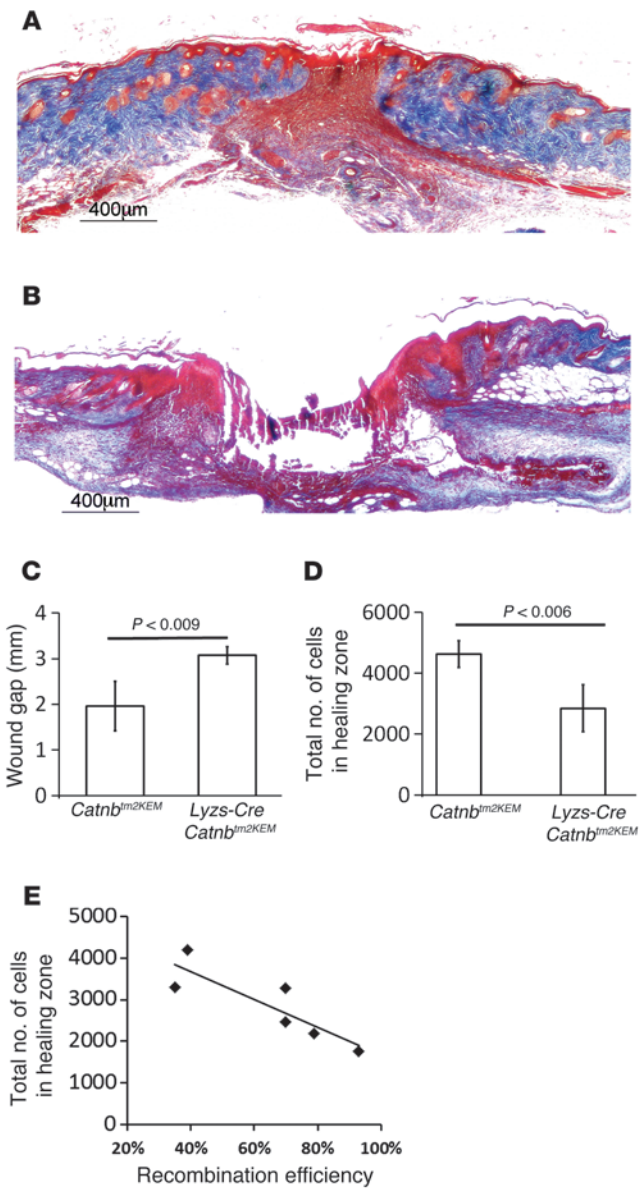

Figure 3
Wounds from mice lacking β-catenin in macrophages do not heal. Trichrome-stained histology of healing wounds. Seven days after wounding, there was a lack of cells in the region that normally contains wound granulation tissue in *Lysz-Cre Catnb*^{tm2KEM} mice (lacking β-catenin in myeloid cells) compared with that seen in their control littermates. (**A**) Representative histologic section of a healing wound in a control mouse. Scale bar: 400 μm. (**B**) Representative histologic section of a healing wound in a mouse in which β-catenin was depleted from macrophages. Scale bar: 400 μm. (**C**) Wound gap measurements show a larger gap in the *Lysz-Cre Catnb*^{tm2KEM} mice compared with that seen in control mice. (**D**) Cell density quantification shows a significant decrease in the number of cells in a healing wound in *Lysz-Cre Catnb*^{tm2KEM} mice compared with the number of cells observed in control mice. (**E**) The percentage of bone marrow–derived EYFP-positive macrophages in *Lysz-Cre Catnb*^{tm2KEM} *ROSA-EYFP* mice inversely correlated with the total number of cells in the healing wound (correlation coefficient = –0.865, $P < 0.014$).

β-catenin demonstrated less migration into the cell-denuded gap than did control macrophages (Figure 6, A and B). Using a Boyden chamber Transwell migration assay, we measured the number of macrophages migrating through a porous membrane to reach a monolayer of murine fibroblasts (Figure 6C) or a fibroblast-free cell culture surface (Figure 6D). In both situations, the number of β-catenin–deficient macrophages migrating across the membrane was significantly lower than the number of control macrophages.

β-*Catenin regulates TGF-β1 production in macrophages during wound repair*. Macrophages during wound repair liberate TGF-β1 (15, 33–35). To evaluate whether β-catenin signaling affects active TGF-β1 production by macrophages, we compared macrophages obtained from the bone marrow of *Lysz-Cre Catnb*^{tm2KEM} *ROSA-EYFP* mice with those from control *Catnb*^{tm2KEM} *ROSA-EYFP*. β-catenin–deficient macrophages displayed significantly lower levels of TGF-β1 compared with control macrophages (Figure 7A). Using a reporter cell line that produces luciferase under the control of a PAI-1 promoter, we found that conditioned media from β-catenin–deficient macrophages induced less TGF-β1 signaling in fibroblasts compared with that in the media from control macrophages. Direct cocultures with fibroblasts and β-catenin–deficient macrophages exhibited substantially lower active TGF-β1 signaling compared with that in control macrophages, as detected by the number of pSmad2-positive cells in fibroblasts (Figure 7, B and C). The percentage of Ki67-positive proliferating fibroblasts was also lower in coculture with β-catenin–deficient macrophages than with control macrophages (Figure 7, D and E). To determine whether this decrease in TGF-β1 signaling by β-catenin macrophages plays a functional role in the defective wound repair, we treated wounds from β-catenin–deficient mice with recombinant TGF-β1. Treatment with TGF-β1 increased the number of cells in the wound granulation tissue (Figure 7F, $P < 0.01$) and resulted in a healing phenotype that is closer to that observed in the normal healing situation (Figure 7, G and H).

β-*Catenin is required for a subpopulation of lysozyme-expressing cells to attain a mesenchymal cell–like phenotype*. Macrophages are thought to have the capacity to attain cytological features similar to those in mesenchymal cells (36–41). Such a phenotype might be related to their migratory capacity, as is the case in tumor cells during migration (8, 32, 42). EYFP-positive cells in 1-week-old wounds were stained for fibroblast activation protein (FAP) (43); a myofibroblast marker, α-smooth muscle actin (α-SMA) (44); and the macrophage marker F4/80 (45). The majority of EYFP-positive cells (57 ± 9%) expressed F4/80 (Supplemental Figure 4A). However, 33 ± 12% of EYFP-positive cells expressed FAP, and 24 ± 9% of EYFP-positive cells expressed α-SMA (Supplemental Figure 4, B and C). To determine whether these findings were related to macrophage clearance of mesenchymal cells or to the ability of macrophages themselves to achieve a fibroblastic phenotype, we examined macrophages in vitro in the absence of mesenchymal cells. A subpopulation of macrophages from *Lyzs-Cre ROSA-EYFP* mice were grown in cell culture, deprived of macrophage differentiation medium, and instead grown in DMEM. These cells developed a phenotype similar to that of fibroblasts (Supplemental Figure 6, A and B), accompanied by an increase in *Axin2,* a target of β-catenin/Tcf signaling (Supplemental Figure 6, C and D), showing that macrophages can attain a mesenchyme-like phenotype in the absence of mesenchymal cells. To determine whether β-catenin plays a

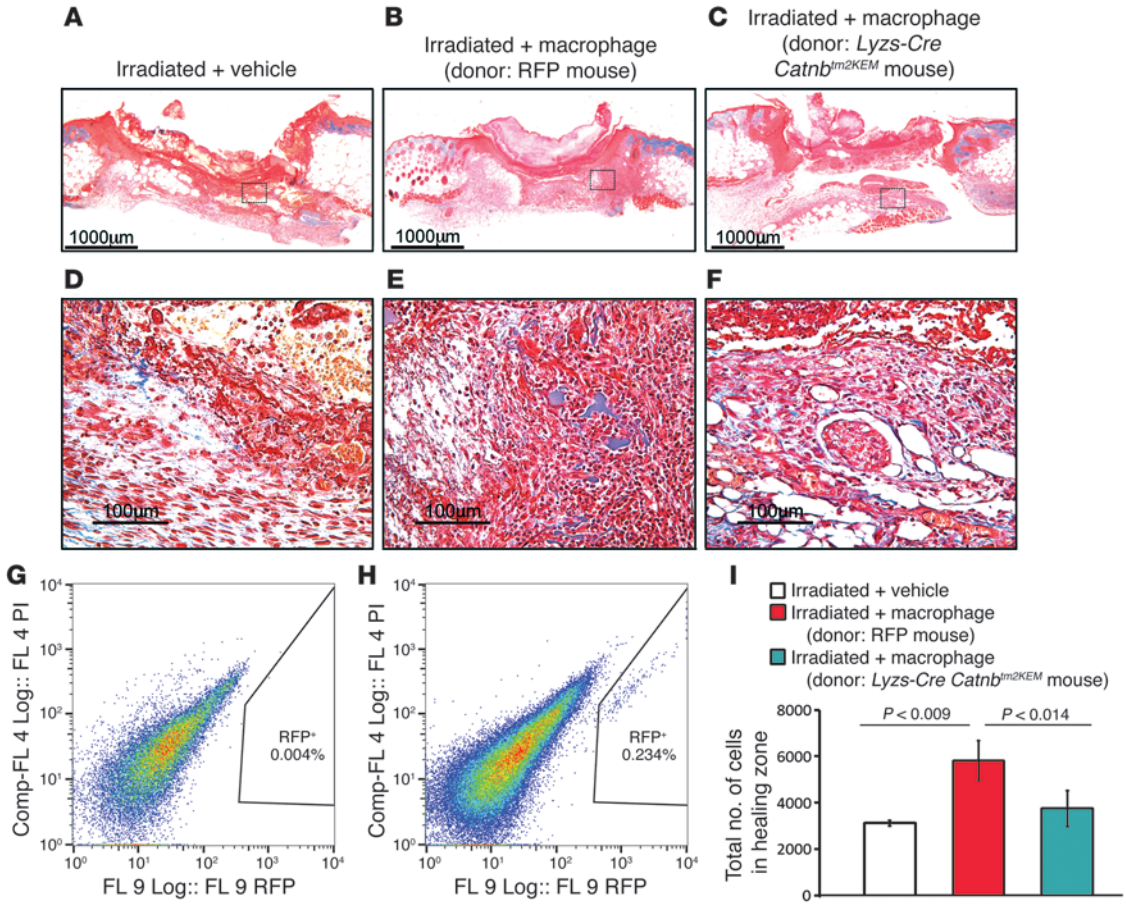

Figure 4

Macrophages deficient in β-catenin cannot rescue deficient wound healing in irradiated mice. Representative histology of healing wounds from an irradiated mouse treated with macrophages from a donor mouse showing partial rescue of the wound phenotype and a significant increase in the number of cells in the wound (**A**–**C** are low-magnification images; scale bars:1,000 μm. **D**–**F** are higher-magnification images; scale bars: 100 μm). Macrophages lacking β-catenin were not able to rescue the phenotype. (**A** and **D**) Irradiated control mouse treated with carrier only. (**B** and **E**) Irradiated mouse treated with macrophages obtained from the bone marrow of a control mouse. (**C** and **F**) Irradiated mouse treated with macrophages from *Lysz-Cre Catnb*^{tm2KEM} mice lacking β-catenin. RFP-labeled macrophages were absent in the healing tissue of control-treated mice (**G**), while they were present in the healing tissue (**H**) of the treated mice 1 week after wounding. (**I**) Quantification of the total number of cells in the healing zone in the various mouse wounds. Data are from 8 mice and are shown as the mean ± 95% CI. Comp-FL, compensated fluorescence.

role in mediating the development of this fibroblastic phenotype, once deprived of macrophage differentiation medium, macrophages from *Lyzs-Cre Catnb*^{tm2KEM} *ROSA-EYFP* and *Lyzs-Cre ROSA-EYFP* mice were grown under identical cell culture conditions. We found that macrophages lacking β-catenin did not develop a fibroblast-like phenotype (Supplemental Figure 6, E and F) and that fibroblasts from these same mice exposed to macrophage-specific media did not express macrophage markers or EYFP in vitro, suggesting that the expression of these markers is not a function of the media used (Supplemental Figure 7).

Macrophage numbers correlate with β-catenin level, cellularity, and scar size in human wound repair. To determine the contribution of macrophages to wound healing in patients, we examined 10 human hypertrophic scars and 3 normal scars (ref. 46 and Supplemental Figure 8). The scar tissues were obtained from patients requiring revision surgery, and hypertrophic scars were characterized by the Vancouver Scar Scale (VSS). Hypertrophic scars are known to exhibit high levels of β-catenin, and their dermal layer is composed of fibroblasts that are similar to those observed during the proliferative phase of wound repair.

The wounds were stained for F4/80$^+$ and β-catenin. There were 4 times the number of F4/80$^+$ cells per high-powered field in the hypertrophic scar tissue (12.3% ± 2.4%) compared with the number seen in normal scars (4.0% ± 1.15%). The number of cells per high-powered field positively correlated with the number of β-catenin$^+$ (correlation coefficient = 0.87, 2-tailed probability = 0.026) and F4/80$^+$ (correlation coefficient = 0.89, 2 tailed probability = 0.019) cells. Thus, the number of macrophage cells correlates with scar size and β-catenin levels in human wound repair. Increased numbers of macrophage cells in a wound may contribute to the development of a hyperplastic scar.

Discussion

β-Catenin plays a critical role in skin wound repair by regulating the ultimate size of the scar. We used cell lineage analysis to show that macrophages in wound granulation tissue exhibit β-catenin/

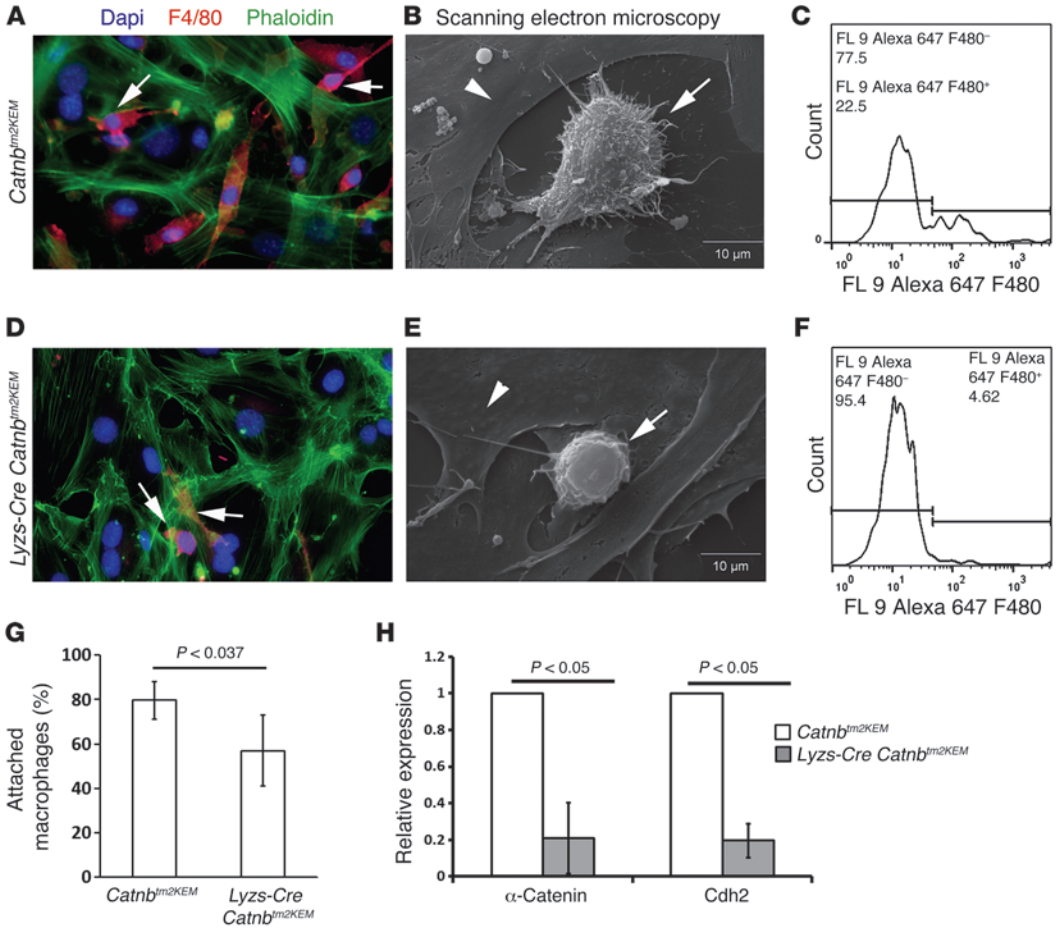

Figure 5

β-Catenin regulates macrophage cell adhesion to fibroblasts. Adhesion assay using control macrophages (**A**–**C**) and macrophages lacking β-catenin (**D**–**F**). Double immunofluorescence staining of macrophages and fibroblasts in cocultures. More F4/80-positive cells were observed in cocultures with control macrophages (**A**) in comparison with macrophages lacking β-catenin (**D**). Arrow shows F4/80-positive cells (red) that remained attached to the fibroblast layer (green). Scanning electron microscopy of macrophages that remained adherent to the fibroblast layer showing that macrophages that lacked β-catenin (**E**) had less pseudopod-like projections in comparison with control macrophages (**B**). Arrows show macrophages, and arrowhead shows fibroblasts. Flow cytometric analysis of washed and trypsinized cultured cells showing that there was a greater decrease in the percentage of F4/80-positive macrophages in macrophages lacking β-catenin (**F**) than in controls (**C**). (**G**) Quantification of the number of attached macrophages on fibroblasts, indicating that fewer macrophages lacking β-catenin adhered to fibroblasts. (**H**) Macrophages lacking β-catenin had lower expression levels of α-catenin and cadherin-2 (N-cadherin) compared with the levels observed in control macrophages. Data represent the mean ± 95% CI for 7 mice.

Tcf signaling activation. By examining cells lacking β-catenin, we found a previously unidentified important function for β-catenin in myeloid lineage cells, that of regulating cell motility and adhesion, and this function is required for normal wound repair.

β-Catenin plays a critical role in regulating the number of macrophages present in the healing wound, and this is likely due to its regulation of cell motility and adhesion. This function of β-catenin is supported by in vitro studies correlating Wnt pathway target genes or β-catenin levels in macrophages with migration and mobilization in response to inflammation (42, 47). β-catenin regulates the expression of genes involved in cell migration and adhesion, such as cadherins, catenins, ADAMs, and integrins, and this gene expression regulation is likely the mechanism by which β-catenin regulates cell motility and adhesion. The importance of macrophage motility and cell adhesion in wound repair is supported by data from mice lacking β2 integrin, in which defective macrophage cell adhesion is associated with poor wound repair (48).

Several factors are known to activate β-catenin during wound healing. Wnt ligands, which activate β-catenin, are present during the earliest phases of wound healing (49). Macrophages express multiple receptors for Wnt, and we identified several in our gene profiling studies (GEO GSE52163). Cytokines liberated early in wound repair can also activate β-catenin. In later phases of repair, extracellular matrix components can regulate β-catenin (50). The excreted factors liberated in early phases of wound healing likely activate β-catenin in macrophages, which in turn regulate the expression of genes that stimulate cell migration to the wound and enhance their adhesion in the region of healing tissues.

During wound healing, macrophages lacking β-catenin produce less TGF-β1 expression, and treatment with TGF-β1 partially

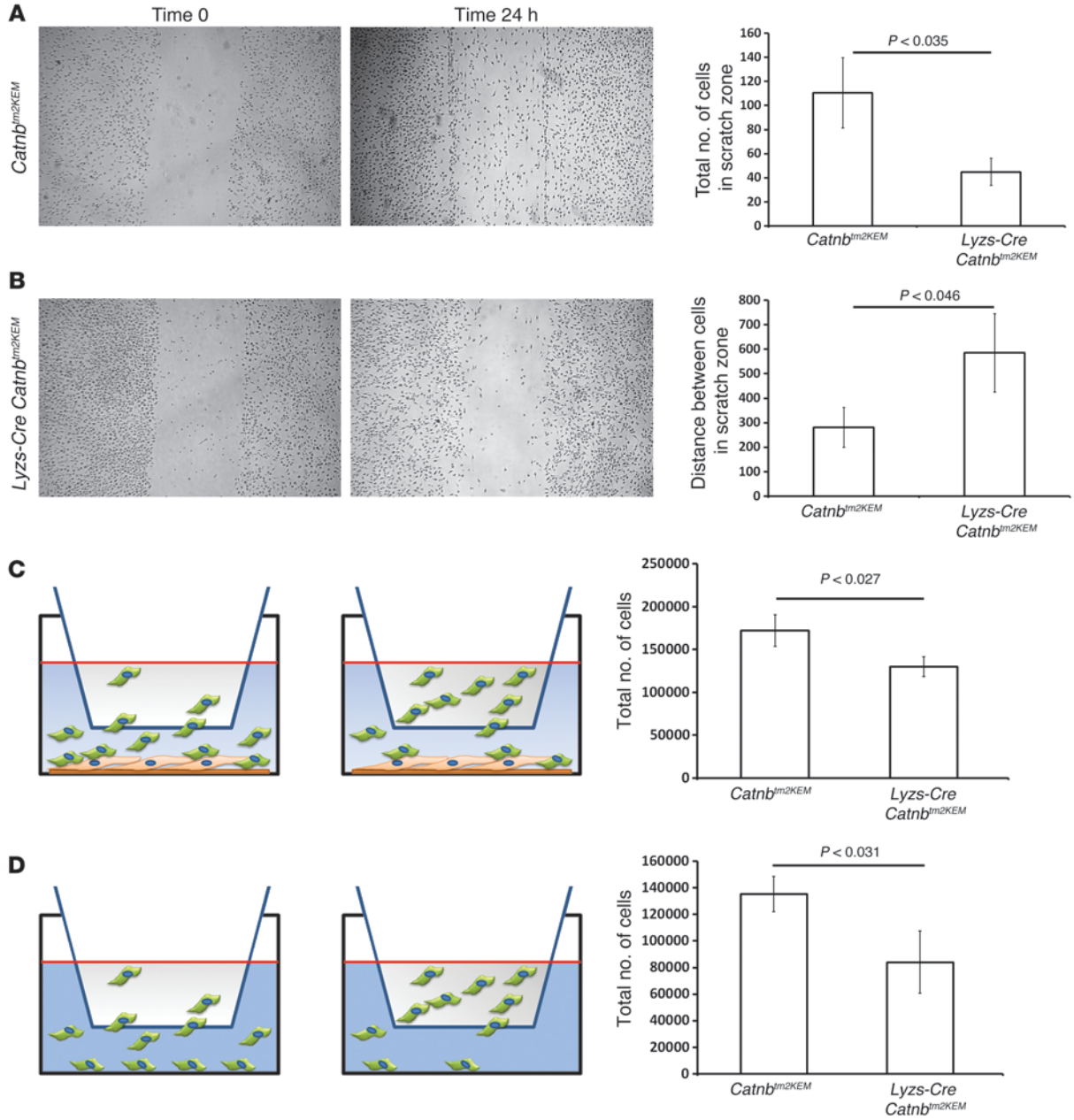

Figure 6

β-Catenin regulates macrophage migration. Representative photomicrographs of a scratch assay performed with (**A**) *Lyzs-Cre ROSA-EYFP* macrophages and (**B**) macrophages from *Lyzs-Cre Catnb*^{tm2KEM} *ROSA-EYFP* mice showing cell migration immediately after scratching and after 24 hours. Migration was quantified by counting the number of cells migrating into the scratch and by measuring the gap. Bar graphs show the means and 95% CI for the number of cells in the scratch zone and the average distance between the 2 edges of the scratch after 24 hours. (**C**) Boyden migration assay with macrophages seeded in the upper chamber and fibroblasts in the lower chamber. The total number of cells in the lower chamber was significantly lower when macrophages from *Lyzs-Cre Catnb*^{tm2KEM} *ROSA-EYFP* mice were used compared with the total number in control macrophages. (**D**) Boyden migration assay using macrophages in the upper chamber, with no cells in the lower chamber. The number of migrated cells in the lower chamber was significantly smaller when macrophages from *Lyzs-Cre Catnb*^{tm2KEM} *ROSA-EYFP* mice were used compared with the number observed in control macrophages. Graphs show the mean ± 95% CI of data from macrophages from 4 mice in each group.

restores normal wound healing in mice lacking β-catenin in macrophages. TGF-β is liberated by macrophages in the wound, and as such, the ability of these cells to migrate to and adhere in granulation tissue is likely responsible for the presence of TGF-β during healing. In support of this notion, macrophages from mice deficient in cd18, which also have impaired adhesion, show decreased TGF-β activity in vitro (48). TGF-β and other cytokines released by macrophages in turn cause mesenchymal cells to populate the healing wound and attain a myofibroblast phenotype (48). Much has been speculated about macrophage cell plasticity, and these

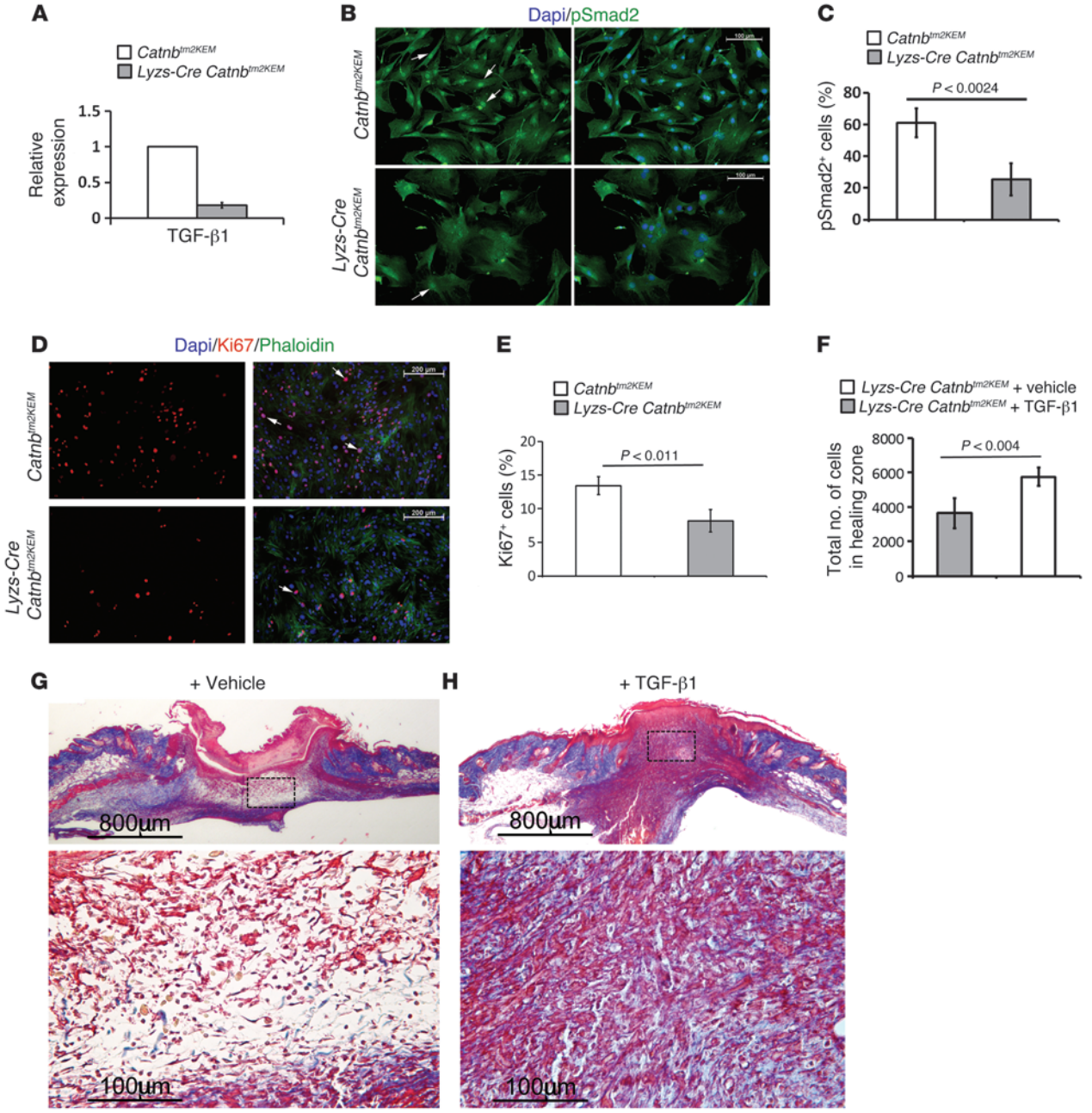

Figure 7

Macrophages lacking β-catenin induce less TGF-β1 signaling, and TGF-β1 partially rescues the wound phenotype of mice lacking β-catenin in macrophages. (**A**) Quantitative RT-PCR analysis showing decreased TGF-β1 expression in β-catenin–deficient macrophages from *Lysz-Cre Catnb*^{tm2KEM} *ROSA-EYFP* mice compared with that seen in their control littermates. (**B**) pSmad2 staining of fibroblasts that were exposed to either control (top panels) or β-catenin–deficient macrophages (bottom panels), indicating less pSmad2-positive cells in fibroblasts that were exposed to macrophages lacking β-catenin (quantified in **C**). Arrow shows pSmad2-positive cells. Scale bars: 100 μm. (**D**) Ki67 staining of fibroblasts that were exposed to either control macrophages (top panels) or to β-catenin–deficient macrophages (lower panels), indicating less Ki67-positive cells in fibroblasts that were exposed to macrophages lacking β-catenin (quantified in **E**). Arrow shows Ki67-positive cells. Scale bars: 200 μm. (**F**) Cell density quantification shows a significant increase in the number of cells in healing wounds in mice treated with TGF-β1 compared with those treated with vehicle. (**G** and **H**) Representative histology of a wound from a mouse treated with vehicle or TGF-β1 whose macrophages lacked β-catenin. Image in **G** is magnified in the lower panel; scale bars: 800 μm; 100 μm. Image in **H** is magnified in the lower panel; scale bars: 800 μm; 100 μm. Data represent the mean ± 95% CI of 7 mice.

cells can attain a fibroblast-like phenotype. Without β-catenin, macrophages are deficient in their ability to achieve this phenotype. In other cell types, migration is related to their ability to achieve a mesenchymal phenotype (8, 32, 42). It is an intriguing possibility that the same notion is true for macrophages. Here, we showed that β-catenin is a critical regulator in macrophage motility and adhesion, and it is likely that adhesion is also required for the release of TGF-β during healing.

β-Catenin is also important in other cell types during healing, and some of this is independent of the role of β-catenin in macrophages. For instance, when only muscle progenitor cells are deficient in β-catenin, there is a smaller wound size (21). When all cell types have lower levels of β-catenin, TGF-β will not cause a dramatic phenotypic rescue in wound repair, as we found when only macrophages were deficient in β-catenin. However, without β-catenin in macrophages, the initial phases of normal healing did not occur. Thus, while β-catenin plays a role in many cell types during repair, its role in the macrophages is essential to initiate the wound process.

In human wound healing, the level and duration of β-catenin activity correlates with wound size (51, 52). In our examination of human wounds, we found that the number of macrophage cells correlates with β-catenin levels, wound cellularity, and scar size, showing the relevance of this pathway and cell type in patients. Several pharmacologic agents are under development that modulate β-catenin activity, and these could be used to treat pathologic wound repair processes. Interestingly, embryonic wounds heal without scarring during stages before the monocyte lineage develops (18), and canonical Wnt signaling, which is active during postnatal healing, is less active in fetal cutaneous wound repair (53). The contribution of Lysz-expressing progeny in wound repair identifies an abundant source of cells that have the potential to be used in patients with deficient wound repair, such as those with irradiated wounds or chronic wounds, and possibly in other repair processes.

Methods

Mice, wounding, and wound analysis. To drive Cre recombinase in Lysz-expressing cells, we used the *Lysz-Cre* (B6.129-Lysz$^{tm1(cre)Ifo}$/J) (24) mouse, which expresses Cre recombinase driven by the endogenous *Lysz* regulatory elements. The *ROSA-EYFP* (B6.129X1-Gt[ROSA]26Sor$^{tm1(EYFP)Cos}$/J) (54) mouse contains an *EYFP* gene inserted into the Gt(ROSA)26Sor locus. Expression of EYFP is inhibited by an upstream LoxP-flanked stop sequence. When bred into mice expressing a Cre recombinase, the stop sequence is deleted and EYFP is expressed. *Catnb^{tm2KEM}* mice (55) possess LoxP sites flanking introns 1 and 6 of the gene encoding β-catenin, resulting in a null allele when exposed to Cre recombinase. Tcf reporter mice (5) contain a *LacZ* gene downstream of a *c-fos* minimal promoter and 3 consensus Tcf-binding motifs. To label cells from donor mice, we used a mouse that constitutively expresses RFP (56). At least 6 mice were used in each group for each experiment (unless otherwise specified), and in experiments in which wound phenotypes were compared, we used a minimum of 8 mice in each group.

To generate full-thickness skin wounds, 3-month-old mice were anesthetized, and the dorsal skin was shaved. After sanitizing with 70% ethanol, 4 full-thickness wounds were created on the dorsal skin using 4-mm-diameter dermal biopsy punches (Miltex Inc.). Wound tissues were excised from mice 1 week after wounding or 4 weeks after wounding, fixed in 10% formalin overnight, and prepared for histologic analysis. To measure scar width, paraffin sections stained with trichrome were used. Intact dermis stains blue when using trichrome staining, since it is a collagen-rich area in comparison with newly formed granulation tissue. This makes a landmark for detecting the wound margin for measurement. Scar size was determined using histologic sections cut at a right angle to the skin surface across the healing wound. Serial sections were observed, and the section with the largest diameter at the center of the healing wound was selected for measurement of the broadest width of the wound. The area of the granulation tissue and the diameter of the wound were measured from the slides, and Meazure 2.0 software (C Thing Software) was used as an aid in measuring the wound diameter, in counting the number of granulation tissue cells, and in measuring the area of the granulation (or dermal) component of the healing wound. To semiquantitatively assess the degree of collagen deposition in the tissue, a modified Masson's trichrome procedure was used and quantified as previously reported (57). Following mordant in Bouin's solution for 20 minutes at 56°C, sections were stained with phosphotungstic-phosphomolybdic acid for 5 minutes, aniline blue dye for 8 minutes, and 1% acetic acid for 2 minutes. The degree of blue staining (collagen deposition score) in the dermis layer was scored from 0 to 10 by 2 independent, blinded observers.

Isolation and culture of bone marrow–derived macrophages. Macrophages were isolated from the bone marrow as previously described (58). Briefly, bone marrow was flushed using lymphocyte medium (RPMI-1640 plus 10% FBS plus 1% penicillin-streptomycin) supplemented with 20 mM HEPES. Cells were then seeded at a concentration of 2×10^6 cells/ml. Conditioned medium from L929 cells (CCL-1, macrophage medium; ATCC) was used to facilitate the growth of macrophages (58).

Macrophage treatment of irradiated wounds. To study deficient wound repair, control mice were exposed to 2.6-Gy whole-body irradiation using a ^{137}Cs irradiator and were wounded 24 hours after irradiation. Cultured macrophages (10^5 cells) from donor mice of the various genotypes were mixed with 50 μl of Matrigel (BD Biosciences) and applied to wounds of recipient mice immediately after injury. RFP mice were provided by Andras Nagy (Samuel Lunenfeld Research Institute, Mount Sinai Hospital, Toronto, Canada).

TGF-β1 treatment of the wounds. Recombinant TGF-β1 (500 ng; Sigma-Aldrich) was mixed with 50 μl Matrigel and applied to each wound in the recipient mice immediately after injury.

Immunohistochemical analysis. Histologic sections were analyzed using immunohistochemistry with antibodies against GFP (Rockland Inc.); F4/80 (Serotec); Mac1, FAP, α-SMA, and β-gal (all from Abcam); β-catenin, pSmad2, and Ki67 (all from Cell Signaling Technology); and involucrin and phalloidin (both from Invitrogen). The antibodies were detected using a biotinylated secondary antibody, and sections were counterstained using DAPI. Five high-powered fields were examined at identical intervals across the healing wound to count the number of cells with positive and negative staining for each sample. AxioVision software (Zeiss) was used to assist in the cell counting. LacZ expression was detected by incubating wound samples in 5-bromo-4-chloro-3-indolyl β-D-galactosidase staining solution according to a protocol obtained from Specialty Media (5). For human tissue staining (10 hypertrophic scar samples and 3 normal scars), we used the Betazoid DAB chromogen kit (Biocare Medical) according to the manufacturer's protocol. For quantifications, 5 high-powered fields were examined at identical intervals across the dermal components of scars to count the number of cells with positive and negative staining for each marker. Human scar tissues were provided by Marc G. Jeschke (Ross Tilley Burn Centre, Sunnybrook Health Science Center, Toronto, Canada).

Gene expression analysis. The healing wound was dissected from the unwounded tissue using microdissection. Healing wound tissue was homogenized, total RNA was extracted, and reverse transcription was performed to generate cDNA, which was analyzed using real-time PCR with specific primers purchased from Life Technologies (59). To compare β-gal–positive cell expression data with β-gal–negative cells, gene expression analysis was performed using Parktec Genotyping Suite and Ingenuity Systems

Software. RNA from these cell populations was analyzed using microarray. In addition, total RNA of bone marrow–derived macrophages from *Lysz-Cre Catnb^{tm2KEM}* mice and control macrophages from *Catnb^{tm2KEM}* mice were extracted using a QIAGEN kit according to the manufacturer's instructions, and expression profiles were compared using microarray analysis.

For gene profile analysis, RNA quality was assessed with a Bioanalyzer (Agilent Technologies), and samples with an RNA integrity number (RIN) greater than 8.5 were included for array. cDNA was generated and hybridized onto the Affymetrix Mouse Gene 1.0 ST chips. Analysis of gene expression was performed using Parktec Genotyping Suite and Ingenuity Systems Software.

Flow cytometry. Microdissected healing wounds were used for cell analysis. Briefly, the scar was chopped into fine pieces, then transferred to a warmed collagenase cocktail (1X dispase, 0.05% trypsin, 1,000 U collagenase in high-glucose DMEM with 1% antibiotic-antimycotic). The collagenase cocktail with tissue was rotated at 37°C for up to 30 minutes. Halfway through incubation, the tissue was gently passed through a syringe with a 16-gauge needle to aid in breaking down the tissue. Once digested, the cocktail was filtered through a 100-μm filter, centrifuged for 5 minutes at 150 *g*, and the supernatant was removed. The cell pellet was resuspended in growth medium, counted, and separated equally into flow tubes. For flow cytometry of β-gal–positive cells, the dissociated cells were fixed and permeabilized using BD Cytofix/Cytoperm buffer for 20 minutes at room temperature. After washing, cells were resuspended in staining buffer containing FDG (60) substrate, which gives a green fluorescent product to cells expressing β-gal. MoFlow (Cytomation) with a 488-nm blue laser power set to 100 mW and FL1 with a 530/40 BP filter were used to select EYFP-expressing cells.

Adhesion assay. Fibroblasts were cultured at 15,000 cells/cm^2 for 4 days. 20,000 macrophages/cm^2 in 1 ml of media (10% FBS, DMEM, 1% penicillin-streptomycin) were added on the fourth day for 6 hours. The supernatant was collected, and the number of nonadherent macrophages was counted using a Beckman Z1 Coulter Particle counter. Particles between 10 to 20 μm in size were counted to eliminate any potentially detached fibroblasts.

Scanning electron microscopy. Scanning electron microscopy was used to examine the morphological characteristics of macrophages in adhesion assays. Cells were fixed in 2% glutaraldehyde in 0.1 M sodium cacodylate (pH 7.3). After washing in buffer, cells were dehydrated in a graded series of ethanol solutions. After critical-point drying (Bal-Tec CPD 030), the samples were sputtered with gold (Denton Desk II sputter coater), and the probes were examined by scanning electron microscopy (FEI XL30 ESEM; Philips). Macrophages from 3 β-catenin–deficient mice (*Lyzs-Cre Catnb^{tm2KEM} ROSA-EYFP*) and 3 control (*Lyzs-Cre ROSA-EYFP*) mice were analyzed.

Migration and invasion assays. Bone marrow–derived monocytes were grown in macrophage-inducing medium to a confluence of 80% to 100% before the cell monolayer was scratched using a sterile micropipette tip. After washes with PBS, fresh macrophage-specific medium was added. The images of the wounded area were captured immediately after the scratch (*t*0) and 24 hours later (*t*24) to monitor macrophage migration into the wounded area. The migratory abilities were quantified by measuring the total number of cells in the scratched regions as well as by measuring the distance between cells in the scratch zone.

Invasion assays were performed using a Boyden Chamber CytoSelect Cell Migration Assay kit with polycarbonate membrane inserts (5-μm pore size; Cell Biolabs Inc.). Bone marrow–derived macrophages (10^5 cells) were placed inside the insert containing macrophage-specific media. A coverslip pre-seeded with 10^5 control fibroblasts was placed at the bottom of the lower chamber. Macrophages were allowed to migrate for 6 hours before the upper chamber was removed. The total number of macrophages in the lower chamber (adhered and floating cells) was quantified, and the same approach was used in the experiment set up without fibroblasts in the lower chamber.

Statistics. Data are presented as the mean ± 95% CI, unless otherwise specified. A 2-tailed Student's *t* test and Pearson's correlation coefficient test were used for analysis. A *P* value less than 0.05 was considered statistically significant. To estimate the sample size for mouse studies, we performed a power calculation to determine the number of animals that would be needed in each group to detect a 25% difference in scar size based on the mean scar size and the variability from our previous studies (10, 21). We calculated that 8 mice would be needed in each group to detect this difference.

Study approval. All procedures using animals were approved by the Sick Kids animal care committee (7014; March 19, 2009) under the auspices of the Canadian Council on Animal Care. Human tissue samples were obtained following provision of informed consent from the patients who were undergoing reconstructive burn surgery. The scar tissues were obtained (approval 194-2010) from patients requiring revision surgery, and hypertrophic scars were characterized by the VSS (61). Vascularity, pigmentation, pliability, and height were measured according to the VSS.

Acknowledgments

We wish to thank Jalil Hakimi, Huimin Wang, Michelle Tseng, and Sherry Zhao for their technical assistance. This work was supported by grants from the Canadian Institutes of Health Research (CIHR) (FRN 62788, to B.A. Alman). S Amini-Nik is supported by the Ontario Institute for Cancer Research. The work of B. Hinz and E. Cambridge was supported by the CIHR (210820 and 286920); the Collaborative Health Research Programme (CIHR/NSERC) (1004005 and 413783); and the Canada Foundation for Innovation and Ontario Research Fund (CFI/ORF) (26653).

Received for publication May 3, 2013, and accepted in revised form March 27, 2014.

Address correspondence to: Benjamin A. Alman, Department of Orthopedic Surgery, Duke University, 200 Trent Drive, Durham, North Carolina 27710, USA. Phone: 919.613.6935; Fax: 919.613.6991; E-mail: ben.alman@duke.edu.

1. Sen CK, et al. Human skin wounds: a major and snowballing threat to public health and the economy. *Wound Repair Regen*. 2009;17(6):763–771.
2. Gottrup F. A specialized wound-healing center concept: importance of a multidisciplinary department structure and surgical treatment facilities in the treatment of chronic wounds. *Am J Surg*. 2004;187(5A):38S–43S.
3. Gurtner GC, Werner S, Barrandon Y, Longaker MT. Wound repair and regeneration. *Nature*. 2008;453(7193):314–321.
4. Bielefeld KA, Amini-Nik S, Alman BA. Cutaneous wound healing: recruiting developmental pathways for regeneration. *Cell Mol Life Sci*. 2013; 70(12):2059–2081.
5. Cheon SS, et al. β-Catenin stabilization dysregulates mesenchymal cell proliferation, motility, and invasiveness and causes aggressive fibromatosis and hyperplastic cutaneous wounds. *Proc Natl Acad Sci U S A*. 2002;99(10):6973–6978.
6. Amini-Nik S, et al. Ultrafast mid-IR laser scalpel: protein signals of the fundamental limits to minimally invasive surgery. *PLoS One*. 2010;5(9):e13053.
7. Hinz B, et al. Recent developments in myofibroblast biology: paradigms for connective tissue remodeling. *Am J Pathol*. 2012;180(4):1340–1355.
8. Radisky DC, Kenny PA, Bissell MJ. Fibrosis and cancer: do myofibroblasts come also from epithelial cells via EMT? *J Cell Biochem*. 2007;101(4):830–839.
9. DiPietro LA, Burdick M, Low QE, Kunkel SL, Strieter RM. MIP-1α as a critical macrophage chemoattractant in murine wound repair. *J Clin Invest*. 1998;101(8):1693–1698.
10. Cheon SS, et al. β-Catenin regulates wound size and mediates the effect of TGF-β in cutaneous healing. *FASEB J*. 2006;20(6):692–701.
11. Bielefeld KA, et al. Fibronectin and β-catenin act in a regulatory loop in dermal fibroblasts to modulate cutaneous healing. *J Biol Chem*. 2011; 286(31):27687–27697.
12. Harada N, et al. Intestinal polyposis in mice with a dominant stable mutation of the beta-catenin gene. *EMBO J*. 1999;18(21):5931–5942.
13. van Amerongen R, Nusse R. Towards an integrated view of Wnt signaling in development. *Development*. 2009;136(19):3205–3214.
14. Geissmann F, Manz MG, Jung S, Sieweke MH, Merad M, Ley K. Development of monocytes, macrophages,

and dendritic cells. *Science*. 2010;327(5966):656–661.
15. Werner S, Grose R. Regulation of wound healing by growth factors and cytokines. *Physiol Rev*. 2003;83(3):835–870.
16. Goren I, et al. A transgenic mouse model of inducible macrophage depletion: effects of diphtheria toxin-driven lysozyme M-specific cell lineage ablation on wound inflammatory, angiogenic, and contractive processes. *Am J Pathol*. 2009;175(1):132–147.
17. Mirza R, DiPietro LA, Koh TJ. Selective and specific macrophage ablation is detrimental to wound healing in mice. *Am J Pathol*. 2009;175(6):2454–2462.
18. Hopkinson-Woolley J, Hughes D, Gordon S, Martin P. Macrophage recruitment during limb development and wound healing in the embryonic and foetal mouse. *J Cell Sci*. 1994;107(pt 5):1159–1167.
19. Simpson DM, Ross R. The neutrophilic leukocyte in wound repair a study with antineutrophil serum. *J Clin Invest*. 1972;51(8):2009–2023.
20. Leibovich SJ, Ross R. The role of the macrophage in wound repair. A study with hydrocortisone and antimacrophage serum. *Am J Pathol*. 1975;78(1):71–100.
21. Amini-Nik S, Glancy D, Boimer C, Whetstone H, Keller C, Alman BA. Pax7 expressing cells contribute to dermal wound repair, regulating scar size through a β-catenin mediated process. *Stem Cells*. 2011;29(9):1371–1379.
22. Nolan GP, Fiering S, Nicolas JF, Herzenberg LA. Fluorescence-activated cell analysis and sorting of viable mammalian cells based on β-D-galactosidase activity after transduction of Escherichia coli lacZ. *Proc Natl Acad Sci U S A*. 1988;85(8):2603–2607.
23. Chari R, et al. A sequence-based approach to identify reference genes for gene expression analysis. *BMC Med Genomics*. 2010;3:32.
24. Clausen BE, Burkhardt C, Reith W, Renkawitz R, Forster I. Conditional gene targeting in macrophages and granulocytes using LysMcre mice. *Transgenic Res*. 1999;8(4):265–277.
25. Gu Q, Wang D, Cui C, Gao Y, Xia G, Cui X. Effects of radiation on wound healing. *J Environ Pathol Toxicol Oncol*. 1998;17(2):117–123.
26. Tsumano T, et al. A new mouse model of impaired wound healing after irradiation. *J Plast Surg Hand Surg*. 2013;47(2):83–88.
27. Van den Bossche J, et al. Alternatively activated macrophages engage in homotypic and heterotypic interactions through IL-4 and polyamine-induced E-cadherin/catenin complexes. *Blood*. 2009; 114(21):4664–4674.
28. Skokos EA, Charokopos A, Khan K, Wanjala J, Kyriakides TR. Lack of TNF-α-induced MMP-9 production and abnormal E-cadherin redistribution associated with compromised fusion in MCP-1-null macrophages. *Am J Pathol*. 2011;178(5):2311–2321.
29. Van den Bossche J, Van Ginderachter JA. E-cadherin: from epithelial glue to immunological regulator. *Eur J Immunol*. 2013;43(1):34–37.
30. Van den Bossche J, Malissen B, Mantovani A, De Baetselier P, Van Ginderachter JA. Regulation and function of the E-cadherin/catenin complex in cells of the monocyte-macrophage lineage and DCs. *Blood*. 2012;119(7):1623–1633.
31. Allport JR, Muller WA, Luscinskas FW. Monocytes induce reversible focal changes in vascular endothelial cadherin complex during transendothelial migration under flow. *J Cell Biol*. 2000;148(1):203–216.
32. Cai J, et al. MicroRNA-374a activates Wnt/β-catenin signaling to promote breast cancer metastasis. *J Clin Invest*. 2013;123(2):566–579.
33. Hinz B. Formation and function of the myofibroblast during tissue repair. *J Invest Dermatol*. 2007; 127(3):526–537.
34. Wang XJ, Han G, Owens P, Siddiqui Y, Li AG. Role of TGF β-mediated inflammation in cutaneous wound healing. *J Investig Dermatol Symp Proc*. 2006; 11(1):112–117.
35. Poon R, Nik SA, Ahn J, Slade L, Alman BA. β-Catenin and transforming growth factor beta have distinct roles regulating fibroblast cell motility and the induction of collagen lattice contraction. *BMC Cell Biol*. 2009;10:38.
36. Bertrand S, Godoy M, Semal P, Van Gansen P. Transdifferentiation of macrophages into fibroblasts as a result of Schistosoma mansoni infection. *Int J Dev Biol*. 1992;36(1):179–184.
37. Bringuier AF, Seebold-Choqueux C, Moricard Y, Simmons DJ, Milhaud G, Labat ML. T-lymphocyte control of HLA-DR blood monocyte differentiation into neo-fibroblasts. Further evidence of pluripotential secreting functions of HLA-DR monocytes, involving not only collagen but also uromodulin, amyloid-β peptide, α-fetoprotein, and carcinoembryonic antigen. *Biomed Pharmacother*. 1992;46(2–3):91–108.
38. Godoy M, Geuskens M, Van Marck EA, Borojevic R, Van Gansen P. Schistosomiasis and in vitro transdifferentiation of murine peritoneal macrophages into fibroblastic cells. *Parasitol Res*. 1989;76(2):150–161.
39. Labat ML, et al. Monocytic origin of fibroblasts: spontaneous transformation of blood monocytes into neo-fibroblastic structures in osteomyelosclerosis and Engelmann's disease. *Biomed Pharmacother*. 1991;45(7):289–299.
40. Lin ML, Li YP, Li ZR, Lin JX, Zhou XL, Liang D. Macrophages acquire fibroblast characteristics in a rat model of proliferative vitreoretinopathy. *Ophthalmic Res*. 2011;45(4):180–190.
41. Li B, Pozzi A, Young PP. TNFα accelerates monocyte to endothelial transdifferentiation in tumors by the induction of integrin α5 expression and adhesion to fibronectin. *Mol Cancer Res*. 2011;9(6):702–711.
42. Chaffer CL, Weinberg RA. A perspective on cancer cell metastasis. *Science*. 2011;331(6024):1559–1564.
43. Rettig WJ, Garin-Chesa P, Beresford HR, Oettgen HF, Melamed MR, Old LJ. Cell-surface glycoproteins of human sarcomas: differential expression in normal and malignant tissues and cultured cells. *Proc Natl Acad Sci U S A*. 1988;85(9):3110–3114.
44. Jeon ES, et al. Cancer-derived lysophosphatidic acid stimulates differentiation of human mesenchymal stem cells to myofibroblast-like cells. *Stem Cells*. 2008;26(3):789–797.
45. Karnoub AE, et al. Mesenchymal stem cells within tumour stroma promote breast cancer metastasis. *Nature*. 2007;449(7162):557–563.
46. Cheon S, et al. Prolonged β-catenin stabilization and tcf-dependent transcriptional activation in hyperplastic cutaneous wounds. *Lab Invest*. 2005;85(3):416–425.
47. Chou WC, et al. Direct migration of follicular melanocyte stem cells to the epidermis after wounding or UVB irradiation is dependent on Mc1r signaling. *Nat Med*. 2013;19(7):924–929.
48. Peters T, et al. Wound-healing defect of CD18(–/–) mice due to a decrease in TGF-β1 and myofibroblast differentiation. *EMBO J*. 2005;24(19):3400–3410.
49. Labus MB, Stirk CM, Thompson WD, Melvin WT. Expression of Wnt genes in early wound healing. *Wound Repair Regen*. 1998;6(1):58–64.
50. Bielefeld KA, et al. Fibronectin and β-catenin act in a regulatory loop in dermal fibroblasts to modulate cutaneous healing. *J Biol Chem*. 2011; 286(31):27687–27697.
51. Sato M. Upregulation of the Wnt/β-catenin pathway induced by transforming growth factor-beta in hypertrophic scars and keloids. *Acta Derm Venereol*. 2006;86(4):300–307.
52. Yu H, Bock O, Bayat A, Ferguson MW, Mrowietz U. Decreased expression of inhibitory SMAD6 and SMAD7 in keloid scarring. *J Plast Reconstr Aesthet Surg*. 2006;59(3):221–229.
53. Carre AL, et al. Interaction of wingless protein (Wnt), transforming growth factor-β1, and hyaluronan production in fetal and postnatal fibroblasts. *Plast Reconstr Surg*. 2010;125(1):74–88.
54. Srinivas S, et al. Cre reporter strains produced by targeted insertion of EYFP and ECFP into the ROSA26 locus. *BMC Dev Biol*. 2001;1:4.
55. Brault V, et al. Inactivation of the β-catenin gene by Wnt1-Cre-mediated deletion results in dramatic brain malformation and failure of craniofacial development. *Development*. 2001;128(8):1253–1264.
56. Vintersten K, et al. Mouse in red: red fluorescent protein expression in mouse ES cells, embryos, and adult animals. *Genesis*. 2004;40(4):241–246.
57. Amini-Nik S, et al. Ultrafast mid-IR laser scalpel: protein signals of the fundamental limits to minimally invasive surgery. *PLoS One*. 2010;5(9):e13053.
58. Weischenfeldt J, Porse B. Bone Marrow-derived Macrophages (BMM): isolation and applications. *CSH Protoc*. 2008;2008:pdb.prot5080.
59. Amini Nik S, Ebrahim RP, Van Dam K, Cassiman JJ, Tejpar S. TGF-β modulates β-catenin stability and signaling in mesenchymal proliferations. *Exp Cell Res*. 2007;313(13):2887–2895.
60. Plovins A, Alvarez AM, Ibanez M, Molina M, Nombela C. Use of fluorescein-di-β-D-galactopyranoside (FDG) and C12-FDG as substrates for β-galactosidase detection by flow cytometry in animal, bacterial, and yeast cells. *Appl Environ Microbiol*. 1994;60(12):4638–4641.
61. Fearmonti R, Bond J, Erdmann D, Levinson H. A review of scar scales and scar measuring devices. *Eplasty*. 2010;10:e43.